Comparison between vertical shear mixing and surface wave-induced mixing in the extratropical ocean

Fangli Qiao[1] and Chuan Jiang Huang[1]

Received 29 January 2012; revised 20 April 2012; accepted 4 May 2012; published 16 June 2012.

[1] Most parameterizations of vertical mixing are associated with local shear instability, which do not explicitly include the effects of surface waves. Here, we compared the performance of vertical mixing induced by vertical shear of the mean current and that by nonbreaking surface waves in the upper ocean through three numerical experiments. The vertical mixing from vertical shear alone was too weak especially in the extratropical ocean, and failed to produce a reasonable mixed layer depth and seasonal thermocline, which resulted in a large cold bias and an unrealistic seasonal cycle in the subsurface. Surface waves can enhance the vertical mixing in the upper ocean, and induce vertical mixing to sustain a reasonable upper ocean temperature structure especially in the extratropical ocean. Both the temperature structure and seasonal cycle were significantly improved by including the nonbreaking surface wave–induced vertical mixing, no matter whether shear effect was included or not. These results indicate that the vertical mixing from surface waves is more important than that associated with velocity shear of the mean current for the upper ocean especially in the extratropics.

Citation: Qiao, F., and C. J. Huang (2012), Comparison between vertical shear mixing and surface wave-induced mixing in the extratropical ocean, *J. Geophys. Res.*, *117*, C00J16, doi:10.1029/2012JC007930.

1. Introduction

[2] Vertical mixing plays a key role in regulating temperature structure in the ocean. Many parameterizations of vertical mixing have been developed in the past decades, and they are usually associated with local shear instability and buoyancy [e.g., *Pacanowski and Philander*, 1981; *Mellor and Yamada*, 1982; *Large et al.*, 1994]. It is believed that the mixing processes in the tropical ocean are strongly influenced by vertical shear of the mean current [*Crawford and Osborn*, 1979]. Ocean circulation models with these parameterizations can successfully reproduce many general features of the tropical ocean [*Pacanowski and Philander*, 1981].

[3] However, the vertical mixing driven by velocity shear in the extratropical ocean is significantly weaker than that in the tropical ocean [*Li et al.*, 2001]. In the extratropical ocean, dominant mixing mechanism may be different from that in the tropical ocean. Some studies have pointed out that ocean models with shear-dependent mixing schemes failed to produce a reasonable temperature structure in the upper ocean during summer. The simulated sea surface temperature (SST) in the extratropical ocean is too high during summer compared with the observed [*Martin*, 1985], and the subsurface temperature is too low [*Ezer*, 2000]. These systematical biases are usually attributed to insufficient vertical mixing in the upper ocean [*Ezer*, 2000]. Recently, some studies showed that surface waves can effectively amend the problem of insufficient mixing in ocean models [*Qiao et al.*, 2004; *Babanin and Haus*, 2009; *Huang et al.*, 2011; *Pleskachevsky et al.*, 2011; *Shu et al.*, 2011].

[4] The vertical mixing in the ocean is sustained by external mechanical energy input [*Huang*, 1999]. Wind energy input plays a vitally important role in setting up the upper ocean mixing. It is estimated that wind energy input to the geostrophic current is 0.9 TW [*Wunsch*, 1998], and that to the Ekman layer is 3 TW [*Watanabe and Hibiya*, 2002; *Alford*, 2003; *Wang and Huang*, 2004b]. However, wind energy input to surface waves is estimated at 60 TW [*Wang and Huang*, 2004a; *Teng et al.*, 2009], which is much larger than those to the geostrophic current and the Ekman layer.

[5] Most of the wave energy is dissipated locally to influence the vertical mixing through breaking. Measurements revealed that wave breaking causes the dissipation rate of turbulence near the sea surface to be two orders larger than that expected from the classical logarithmic boundary layer [*Agrawal et al.*, 1992; *Drennan et al.*, 1996]. However, the strong mixing associated with wave breaking seems insufficient to improve the simulations of the upper ocean, because it is mainly confined to a thin layer in the order of wave amplitude near the sea surface [*Rapp and Melville*, 1990; *Craig and Banner*, 1994; *Huang et al.*, 2011].

[1]Key Laboratory of Marine Science and Numerical Modeling, First Institute of Oceanography, State Oceanic Administration, Qingdao, China.

Corresponding author: F. Qiao, Key Laboratory of Marine Science and Numerical Modeling, First Institute of Oceanography, State Oceanic Administration, 6 Xianxialing Rd., Qingdao 266061, China. (qiaofl@fio.org.cn; Tel. +86-532-88967400)

[6] Different from wave breaking process, nonbreaking surface waves can directly influence the turbulence in the upper ocean, and then modify the vertical mixing. *Phillips* [1961] pointed out that "Although the use of potential theory has been very successful in describing certain aspects of the dynamics of gravity waves, it is known that in a real fluid the motion can not be truly irrotational." The surface waves, mean current, and turbulence can interact in a variety of ways. Meanwhile, the wave energy can transfer to the turbulence field associated with attenuation of surface waves. Laboratory experiments by *Cheung and Street* [1988] indicated that interaction among the mean current, waves and turbulence fields always occurs in their wind-ruffled mechanically generated wave cases. It is the interaction to cause kinetic energy transfer from the surface wave to the mean current by the wave-induced Reynolds stress, and in turn transfer to turbulence by the turbulence viscosity. Subsequently, these results were confirmed by field experiments [*Anis and Moum*, 1995], which showed similar wave-turbulence interaction in the real ocean when the swells were present. Recently, laboratory experiments by *Babanin and Haus* [2009] and *Dai et al.* [2010] further revealed the existence of turbulence induced by the nonbreaking surface wave. The vertical mixing associated with the nonbreaking surface waves can affect a depth of tens of meters [*Anis and Moum*, 1995] and play an important role in modulating the temperature structure of the upper ocean.

[7] Previous studies showed that the nonbreaking wave–induced vertical mixing can much improve the performances of different vertical mixing parameterization including the Mellor-Yamada scheme [*Lin et al.*, 2006; *Qiao et al.*, 2010] and KPP scheme [*Wang et al.*, 2010; *Shu et al.*, 2011]. In other words, the nonbreaking wave–induced vertical mixing can be added to the mixing from shear instability. In this paper, we attempt to compare the effects of vertical mixings from local velocity shear and from surface waves on the upper ocean using an ocean model, the mixing from shear instability is removed in one numerical experiment. The model and experiments are discussed in section 2. The experiment results are presented in section 3, in which mixing effects from velocity shear and surface waves on the temperature structure and season cycles of the upper ocean are analyzed in detail. Sections 4 and 5 are the discussion and conclusions of this study, respectively.

2. Model Description and Experiments

2.1. The Model Linkage

[8] The Princeton Ocean Model (POM) [*Blumberg and Mellor*, 1987] based on a sigma coordinate is employed in this study. The model domain covers the quasi-global oceans from 72°S to 65°N. The zonal resolution is 1° uniformly. The meridional resolution is 1/3° between 10°S and 10°N, and gradually increases to 1° by 20°N and 20°S. The model has 32 layers in the vertical direction, with at least six layers in the top 60 m and at least 10 additional layers between 60 and 250 m. The topography is obtained from the ETOPO5, with a maximal depth of 5000 m and a minimal depth of 100 m. The topography has been smoothed to minimize pressure gradient errors.

[9] The model integration is started from the WOA01 climatological-mean January temperature and salinity fields [*Conkright et al.*, 2002], and is forced with the climatological monthly mean wind stress taken from the QSCAT/NCEP blended ocean winds from 2000 to 2005 [*Milliff et al.*, 2004] and the climatological monthly mean surface heat flux and freshwater flux [*da Silva et al.*, 1994]. The solar radiation is allowed to penetrate into the ocean with a seawater optical type of Type I [*Paulson and Simpson*, 1977]. Moreover, the SST and sea surface salinity (SSS) are relaxed to the monthly WOA01 climatology, with a relaxation time scales of 48.5 days for SST and 120 days for SSS (for a mixed layer depth of 50 m). Sponge layers are placed along the northern and southern boundaries with 5 rows of grids, in which both temperature and salinity are relaxed toward monthly climatological fields.

[10] The horizontal viscosity and diffusion are calculated by Smagorinsky scheme [*Smagorinsky*, 1963], and the minimum horizontal viscosity is set to 2000 m^2 s^{-1} [*Pezzi and Richards*, 2003]. A time-splitting scheme is used with the barotropic time step of 60 s, and the baroclinic time step of 1200 s.

2.2. Numerical Experiments

[11] In order to compare the effects of vertical mixing from vertical shear and from surface waves on the extratropical ocean, three numerical experiments are carried out. Experiment A (Exp A) is a control run, in which mixing effects from both vertical shear and surface waves are included. The level 2.5 turbulence closure scheme [*Mellor and Yamada*, 1982] is used to calculate the vertical mixing from local shear instability and buoyant. The mixing induced by surface waves, named as B_v, is incorporated into the model through the parameterization by *Qiao et al.* [2004, 2010], which is analytically expressed as

$$B_V = \alpha \iint_{\vec{k}} E(\vec{k}) \exp(2kz) d\vec{k} \frac{\partial}{\partial z} \left[\iint_{\vec{k}} \omega^2 E(\vec{k}) \exp(2kz) d\vec{k} \right]^{\frac{1}{2}} \quad (1)$$

where α is a constant coefficient usually set to be 1, $E(\vec{k})$ represents the wave number spectrum, ω is the wave angular frequency, $\vec{k}$ is the wave number, and z is the vertical coordinate axis (upward positive) with $z = 0$ at the surface.

[12] This parameterization has been successfully incorporated into coastal circulation models [*Xia et al.*, 2006], ocean general circulation models (OGCMs) [*Shu et al.*, 2011], and climate models [*Huang et al.*, 2008], and explained some important phenomena in the oceans [*Lin et al.*, 2006; *Matsuno et al.*, 2006]. The mixing from wave breaking is not included in this experiment because its effect on the upper ocean is insignificant [*Huang et al.*, 2011].

[13] In addition, the background mixing of 1×10^{-4} m^2 s^{-1} (K_{m0}) for viscosity and 1×10^{-5} m^2 s^{-1} (K_{h0}) for diffusivity are added to represent the mixing from internal waves. Then, the vertical viscosity K_m and diffusivity K_h in Exp A are

$$K_m = qlS_m + B_v + K_{m0}, \quad (2a)$$

$$K_h = qlS_h + B_v + K_{h0}, \quad (2b)$$

where $q^2/2$ is the turbulence kinetic energy (TKE), l is a turbulence length scale, and S_m and S_h are stability functions

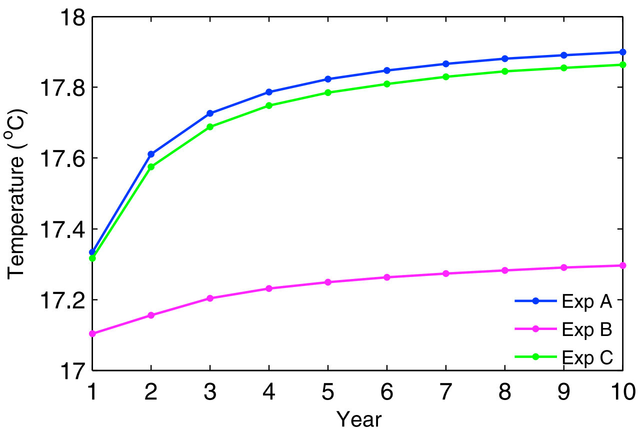

Figure 1. Time evolutions of annual-mean temperature within the upper 200 m averaged between 65°S and 65°N from Exp A (blue, with wave mixing and shear mixing as control run), Exp B (pink, no wave mixing), and Exp C (green, no shear mixing).

[*Mellor and Yamada*, 1982]. Two prognostic equations are solved for q^2 and l as follows,

$$\frac{D}{Dt}\left(\frac{q^2}{2}\right) - \frac{\partial}{\partial z}\left[K_q \frac{\partial}{\partial z}\left(\frac{q^2}{2}\right)\right] = P_S + P_b - \varepsilon, \tag{3a}$$

$$\frac{Dq^2 l}{Dt} - \frac{\partial}{\partial z}\left[Kq\frac{\partial q^2 l}{\partial z}\right] = E_1 l[P_S + E_3 P_b] - l\varepsilon\widetilde{W}, \tag{3b}$$

where K_q is vertical turbulence diffusivity, P_b is buoyant production, $\widetilde{W}$ is a wall proximity function, E_1 and E_3 are nondimensional constants, ε is the TKE dissipation rate, u and v are horizontal velocity components, and

$$P_S = K_m\left[\left(\frac{\partial u}{\partial z}\right)^2 + \left(\frac{\partial v}{\partial z}\right)^2\right] \tag{4}$$

is the shear production of TKE. The MASNUM wave number spectral numerical model [*Yang et al.*, 2005] is employed to compute B_v, and the precalculated monthly mean B_v [*Qiao et al.*, 2004] is used in this numerical experiment.

[14] Exp B is similar to Exp A, but the mixing induced by surface waves was removed, so vertical viscosity K_m and diffusivity K_h are

$$K_m = qlS_m + K_{m0}, \tag{5a}$$

$$K_h = qlS_h + K_{h0}. \tag{5b}$$

In Exp C, the vertical viscosity and diffusivity are also similar as those in Exp A, but the shear effect was removed via setting

$$P_S = 0. \tag{6}$$

Each experiment is integrated for 10 years from the state of rest. Figure 1 shows time evolutions of annual-mean temperature within the upper 200 m simulated in the three experiments. On the whole, the upper ocean in these experiments reaches a quasi-equilibrium state after 5–6 model years. The outputs of the last 3 model years are used to analyze the mixing effects from vertical shear and surface waves in this study.

3. Results

3.1. Mean State in Summer

[15] In winter, the vertical mixing of the upper ocean is dominated by cold convection in the extratropical ocean. In summer, vertical mixing from vertical shear and surface waves become important especially in the extratropical ocean, due to strong surface heat flux that tends to stabilize the upper ocean. So, the analyses in this section will focus on the temperature structure during summer.

[16] Figure 2 shows temperature differences of these three experiments from the climatological data in August along the dateline. In Exp A, the simulated temperature is in agreement with the observation between 20°N and 50°N, with a maximum bias of 1°C, while the temperature is somewhat overestimated below 50 m between 50°N and 60°N (Figure 2a). The mixing of surface waves is removed in Exp B. Compared with Exp A, the most outstanding feature is that its simulated subsurface temperature is significantly underestimated in most areas when compared to the observation, clearly due to insufficient mixing. Its largest bias occurs in the depth

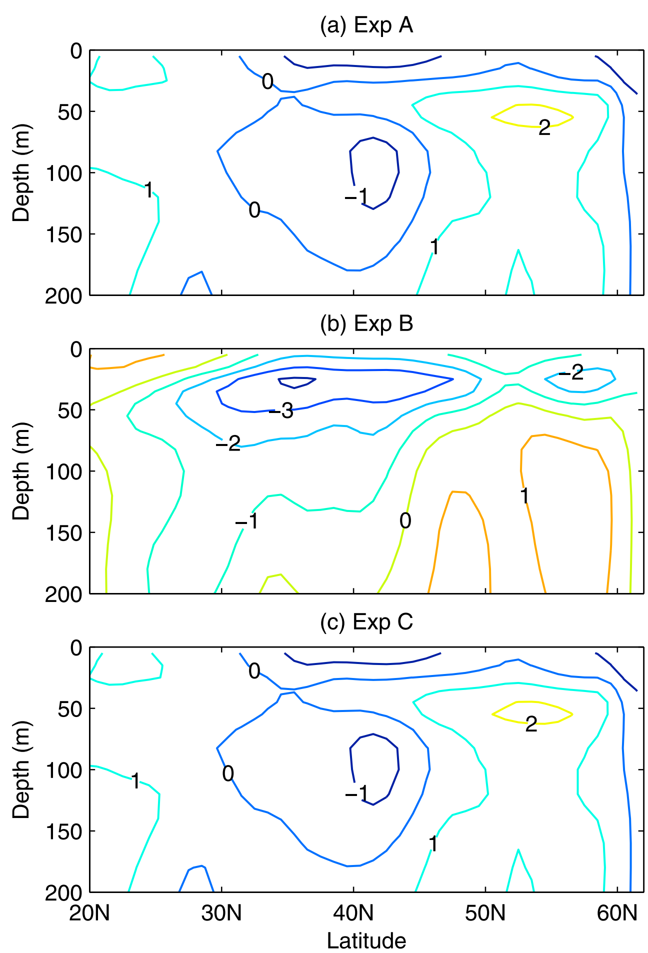

Figure 2. Temperature differences from the climatology averaged in August along the dateline of (a) Exp A, (b) Exp B, and (c) Exp C. Contour interval is 1°C.

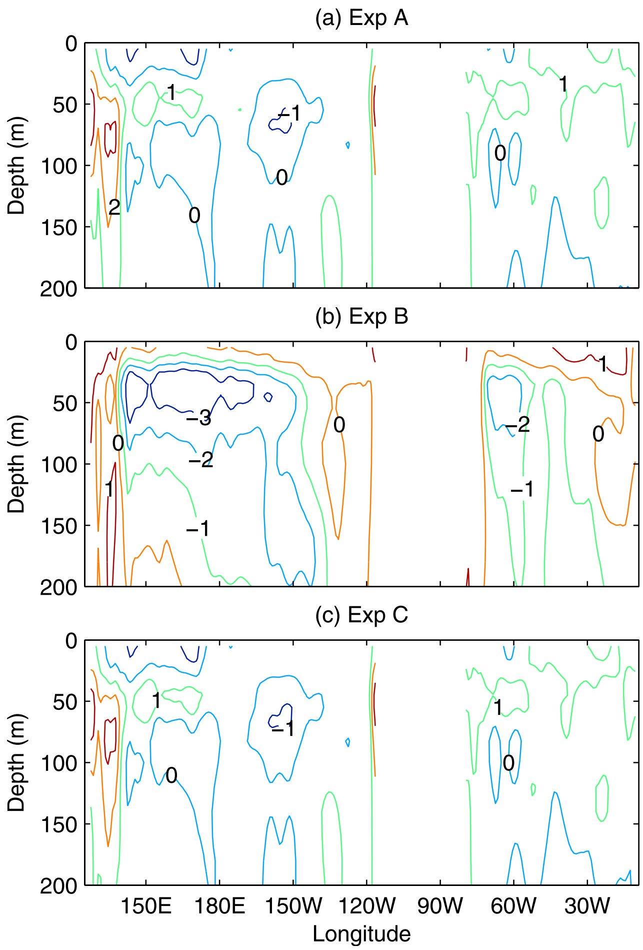

Figure 3. Same as Figure 2, except along 30°N.

range of 20–100 m, with a value of 3°C (Figure 2b). Exp C is the same as Exp A, except that the shear effect on vertical mixing is absent. It is interesting that the simulated temperature in Exp C is very close to that in Exp A. This indicates that the effect of the mean current shear on the upper temperature is insignificant in these regions.

[17] This pattern also appears in Figure 3, which shows temperature differences of the three experiments from the climatological data in August along 30°N. Similar to Figure 2, the biases of temperature in Exp C is very close to those in Exp A. In these two experiments (Exps A and C), the simulated temperature is in good agreement with the observation in the Pacific and Atlantic oceans. However, the simulated subsurface temperature is too cold in Exp B (Figure 3b). In some regions, such as the western boundary of the Pacific Ocean (Figure 3) and the subsurface between 50°N and 60°N (Figure 2), the temperature in all these three experiments has a warm bias, which may be due to the inaccurate simulation of oceanic currents.

[18] The ocean mixed layer depth (MLD) is one of the most important variables in the global climate system because it directly affects the air-sea fluxes of heat, freshwater, carbons dioxide, and many other properties. It is usually shallow in the extratropical ocean during the summer due to the strong solar radiation and relatively weak winds. A weakly stratified layer of water, named as the seasonal thermocline, appears just below the mixed layer. When the effect of surface waves is missing, the mixing driven by vertical shear alone fails to produce a reasonably MLD, as that in Exp B (Figure 4b). The simulated MLD is greatly underestimated in the whole extratropical oceans, compared with that from the climatology (Figure 4d). As a result, the seasonal thermocline is somewhat too shallow and too sharp (Figures 5b and 5d). The too-shallow summer MLD and seasonal thermocline associated to insufficient mixing are a common problem of OGCMs with shear-dependent mixing [*Martin*, 1985; *Ezer*, 2000; *Li et al.*, 2001]. Accordingly, there is a large cold bias in the subsurface (Figures 2b and 3b).

[19] Surface waves can enhance greatly the vertical mixing of the upper ocean, which can transport more heat from the surface to the subsurface. The simulated MLD (Figures 4a and 4c) and seasonal thermocline (Figures 5a and 5c) are greatly improved due to enhanced mixing in the experiments with the effect of surface waves, and the temperature structure is very consistent with that from the climatology.

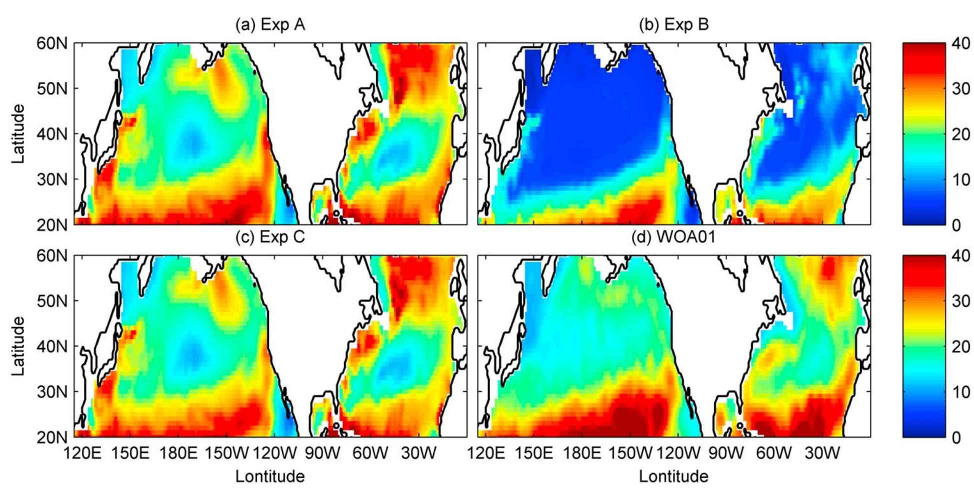

Figure 4. Simulated MLD (units: m) in August from (a) Exp A, (b) Exp B, (c) Exp C, and (d) that from the climatology. The MLD is defined as the depth at which the temperature deviates by 0.2°C for its surface value.

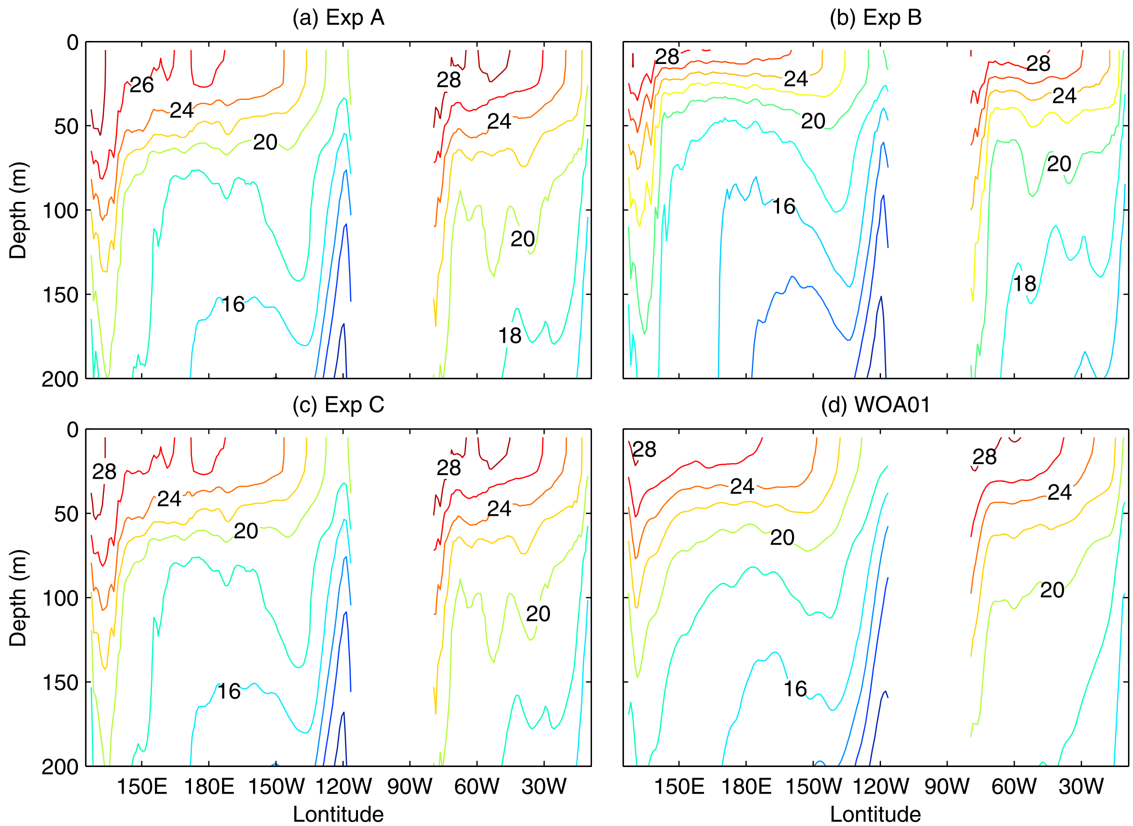

Figure 5. Temperature distribution along 30°N in August from (a) Exp A, (b) Exp B, (c) Exp C, and (d) the climatology. Contour interval is 2°C.

3.2. Seasonal Cycle

[20] In this section, the mixing effects of vertical shear and surface waves are analyzed in terms of seasonal cycle of upper ocean thermal structure. Figure 6 shows the vertical profiles of temperature in the central North Pacific region (30°N and 180°E). Similar to previous studies [e.g., *Ezer*, 2000; *Li et al.*, 2001], the seasonal thermocline in Exp B is too shallow and too sharp due to insufficient vertical mixing. It results in the simulated temperature in summer being somewhat overestimated near the surface, and significantly underestimated in the subsurface. For example, the simulated temperature near the surface is above 27.4°C in August at this location, while the observation is only about 26.5°C. On the other hand, the temperature at the depth of 75 m decreases to about 16.5°C in Exp B, which is much colder than that from the observation (Figure 7).

[21] In Exps A and C, the seasonal thermocline is greatly improved due to enhanced vertical mixing, in which the temperature profile is very close to that from the climatology (Figures 6a, 6c, and 6d). Although Exp C does not include the effect of vertical shear, it has only a negligible difference from that of Exp A. In winter, the simulated temperature is also improved by surface waves. It indicates that the vertical mixing in winter is not completely determined by cooling-induced convection in these regions; surface waves also play a role in the upper thermal distribution in winter.

[22] In Exp B (without the effect of surface waves), the subsurface temperature was too cold to produce a realistic seasonal cycle. The correlation coefficient between the simulated and climatological monthly mean temperature, defined as in *Kara et al.* [2003] and *Wang et al.* [2010], was very small or negative in some regions. Figure 8 shows the profiles of the correlation coefficient in the central North Pacific region (30°N and 180°E) in these three experiments. The correlation coefficient in Exp B is significantly smaller than that in Exps A and C in the most of the depth. The correlation coefficient is negative at some depths in Exp B. This is because its seasonal cycle is reversed from the observed climatology (Figure 9). In these regions, the climatological temperature in summer is somewhat colder than that in winter. Exp B fails to simulate this seasonal cycle due to the shallow thermocline, therefore resulting a negative correlation.

[23] Figure 10 shows the zonally averaged correlation coefficients between the simulated and climatological temperature within the upper 200 m. The correlation coefficients in these three numerical experiments are very close to each other in the tropical region, while they are quite different in the extratropical region. In the extratropical region, the correlation coefficients in Exps A and C are much larger than that in Exp B. For example, the correlation coefficients at 30°N are 0.63 in Exps A and C, while it is only 0.43 in Exp B. This indicates that surface waves play an important role in regulating the season cycle of temperature and thermocline in the extratropical region.

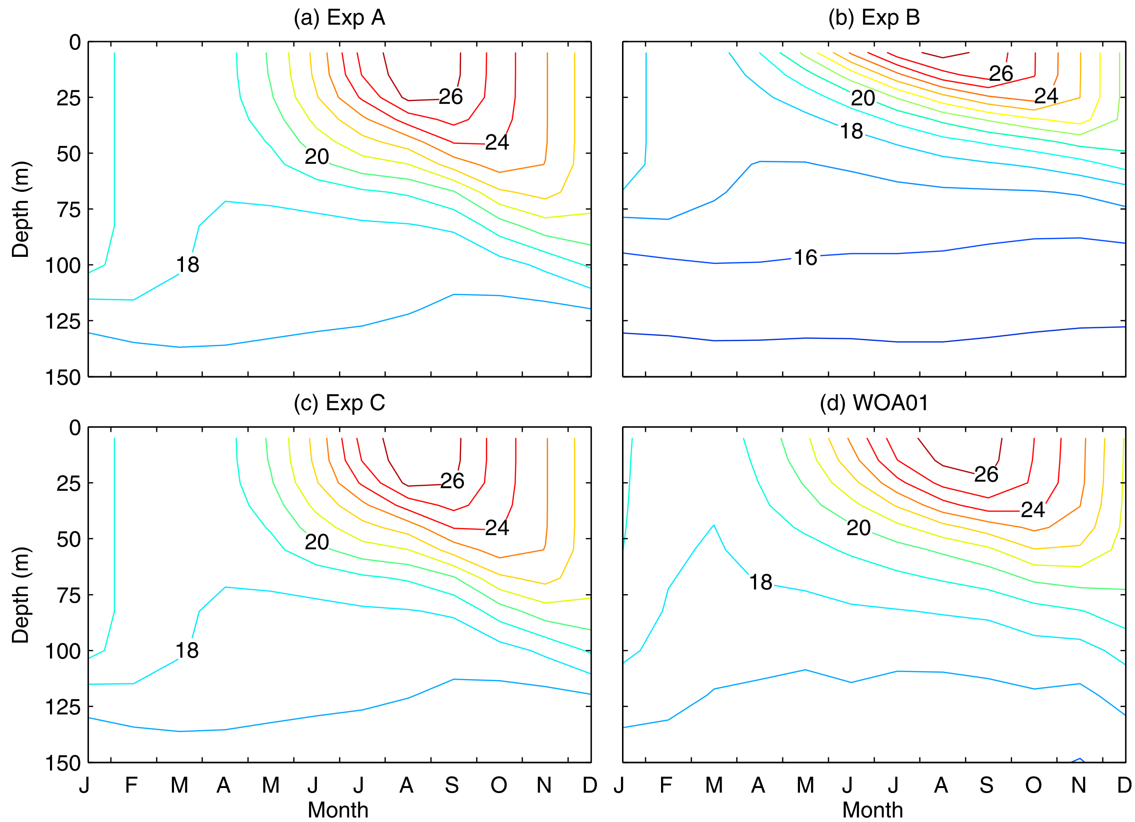

Figure 6. Monthly mean temperature as a function of depth and time at 30°N, 180°E from (a) Exp A, (b) Exp B, (c) Exp C, and (d) the climatology. Contour interval is 1°C.

[24] In all these three experiments, the correlation coefficient near the surface is close to 1.0 (Figure 8). This high correlation results from the following two reasons: First, the SST is sensitive to the mean surface fluxes, rather than the parameterization of vertical mixing [*Chen et al.*, 1994]. Second, the presence of a relaxation term on the surface heat fluxes restricts the development of SST anomalies [*Maes et al.*, 1997]. Then, the seasonal cycle of the temperature near the surface is consistent with the climatology in all three experiments, although the vertical mixing may be greatly different. In these experiments, the most obvious biases occur at the subsurface, while these differences are relatively small near the surface (Figures 2 and 3).

4. Discussion

[25] As can been seen from the above results, the simulated subsurface temperature is significantly underestimated in the experiment without the mixing of surface waves (Exp B).

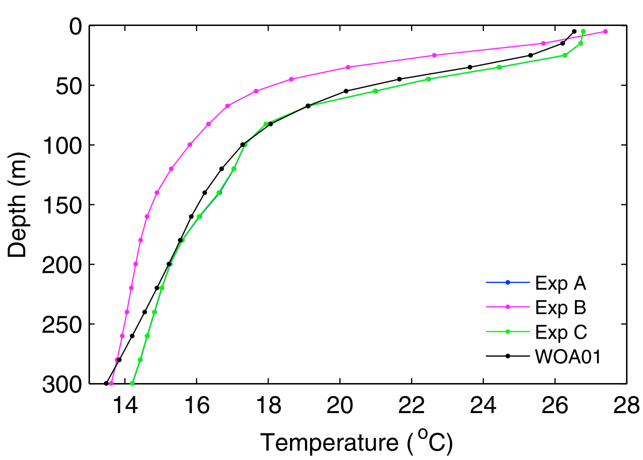

Figure 7. Simulated and climatological temperature profiles in August at 30°N, 180°E.

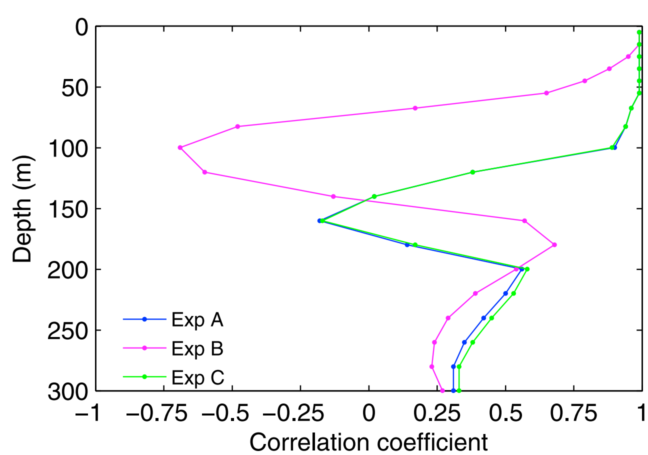

Figure 8. Profiles of correlation coefficient between simulated and climatological monthly mean temperature at 30°N, 180°E.

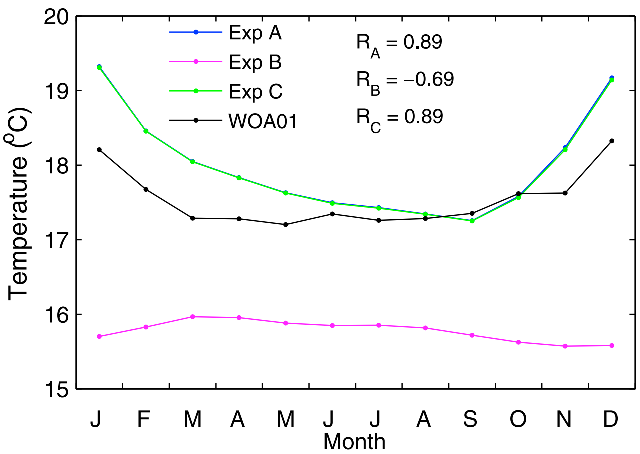

Figure 9. Simulated and climatological monthly mean temperature at 100 m depth at 30°N, 180°E. R is the correlation coefficient between the simulated and climatological temperature.

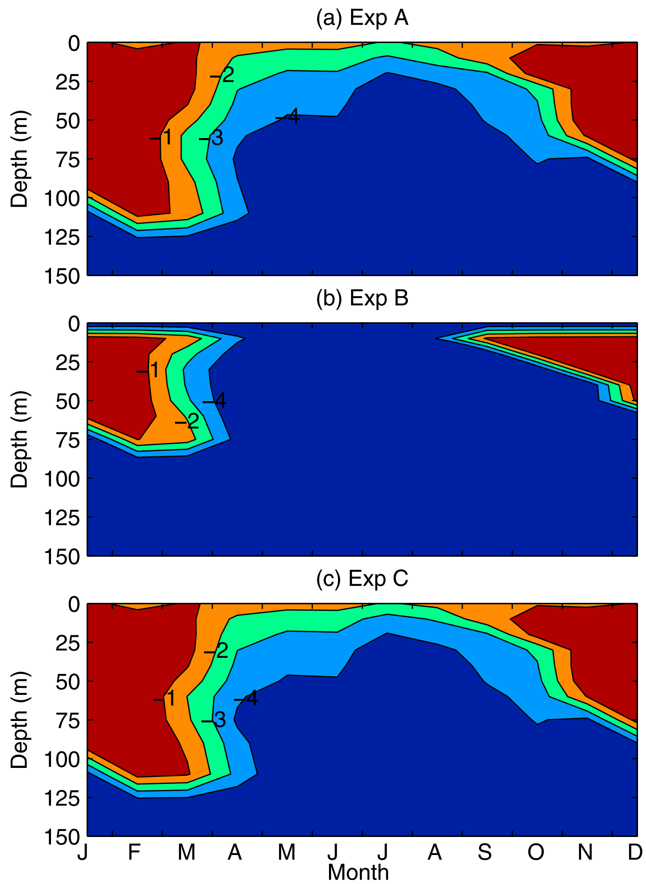

Figure 11. Monthly mean vertical diffusivity as a function of depth and time at 30°N, 180°E from (a) Exp A, (b) Exp B, and (c) Exp C. (The diffusivities have been taken by denary logarithm; units: m^2 s^{-1}.)

This bias is usually attributed to insufficient mixing [*Ezer*, 2000]. The thermal structure is primarily determined by a one-dimensional heat balance due to weak advections in the central gyre region of the extratropics. In the numerical experiment without the effect of surface waves (Exp B), the simulated diffusivity is very close to 10^{-5} m^2 s^{-1} from March to September (Figure 11b), which is nearly the same to the background mixing set standing for the internal waves in the model. This weak diffusivity restrains heat transport from the surface layer to the subsurface, resulting in an unrealistic MLD and seasonal thermocline, then a cold bias in the subsurface.

[26] However, when surface waves are incorporated in the model, even without the mixing from the vertical shear, the temperature distribution of the upper ocean is improved greatly compared with that of the experiment without surface waves. The simulated temperature is consistent with the observation in most regions. These improvements are closely associated with the change in vertical diffusivity (Figure 11).

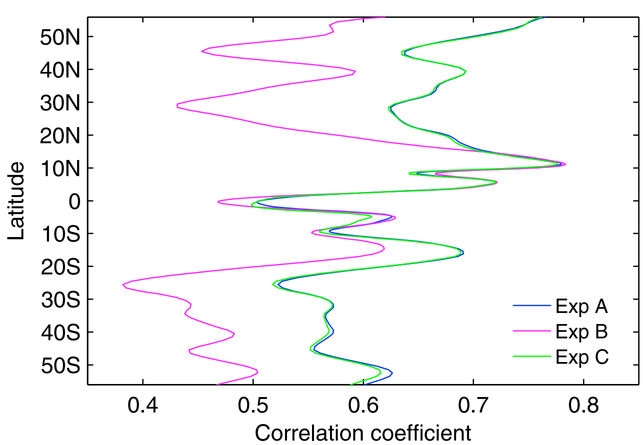

Figure 10. Zonally averaged correlation coefficients between the simulated and monthly mean climatological temperature in the upper 200 m.

[27] Surface waves can greatly enhance the turbulence, and then the vertical mixing. The wave motion, especially the long swells with small wave numbers, can affect greater depths since the surface wave–induced mixing decays much slowly with depth than that of short wave [*Qiao et al.*, 2004]. The observations show that strong turbulence induced by long swells can extend to tens of meters in the oceans [*Anis and Moum*, 1995]. The vertical mixing was greatly enhanced in the experiments with the effects of surface waves (Figures 11a and 11c). The enhanced mixing by surface waves can transport heat more effectively from the surface layer to the subsurface, resulting in an increase of subsurface temperature. As a result, the temperature distribution of the upper ocean is improved greatly.

[28] It is interesting that the simulated temperature in the numerical experiment without the shear effect is very close to that with the shear effect, when surface waves are incorporated into the model. This indicates that the combined mixing from surface waves and buoyancy can sustain a reasonable temperature structure in the upper ocean and that the effect from vertical shear is negligible. During summer, both local winds and horizontal currents are small in most regions of the extratropical ocean (Figure 12). Accordingly, the vertical shear of mean currents is very weak, so that its effect is relatively insignificant.

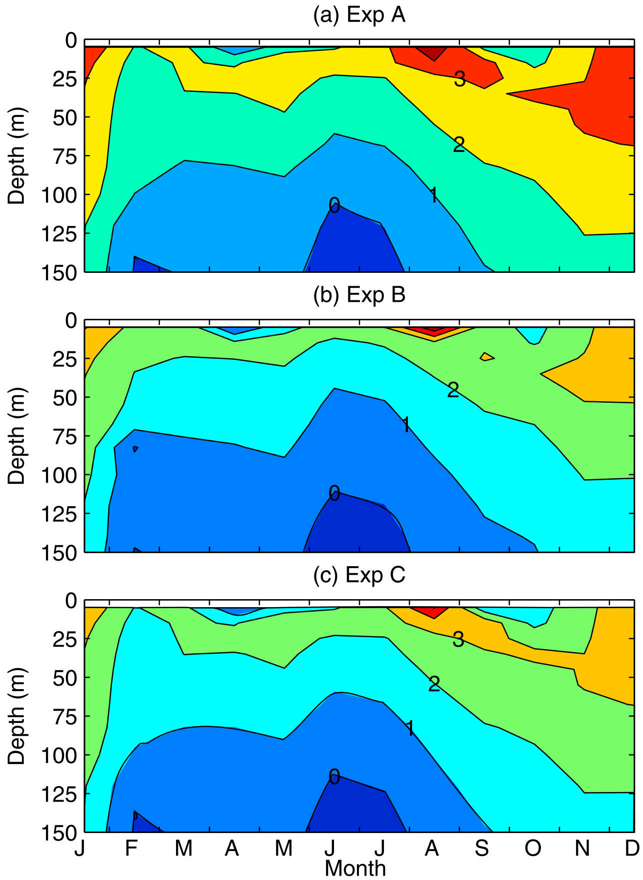

Figure 12. Same as Figure 11, except for zonal velocity. Contour interval is 1 cm s^{-1}.

[29] However, surface waves are not totally determined by local winds. The swells can travel from their generation area, over a long distance across ocean basin. For example, the swells generated in the Southern Ocean can be across the equator and reach to the coast of the North America, and those generated in the central Northern Pacific can propagate to the coasts from Alaska to Hawaii [*Snodgrass et al.*, 1966; *Collard et al.*, 2009]. Along their long path of propagation, the amplitude of the swell is gradually decreasing, in which a significant portion of energy leaks to the ocean via different processes [*Cheung and Street*, 1988; *Anis and Moum*, 1995; *Teixeira and Belcher*, 2002]. Thus, even in the regions with weak winds, surface wave can also play important mixing role through swell.

[30] It should be noted that our result is suitable for the regions with weak currents. In the regions with strong currents and fronts, such as the western boundary of the ocean and the tropical ocean, the velocity shear is relatively large; therefore its induced vertical mixing may be more important than that induced by surface waves.

5. Conclusion

[31] The vertical mixing in the ocean is sustained by external mechanical energy input. Wind energy input to surface waves is the dominant source of external mechanical energy for the ocean. The turbulence produced by surface waves can exert important influence on the vertical mixing of the upper ocean. The influences of vertical mixing induced by vertical shear and surface waves on the extratropical upper ocean were compared through three experiments in this study.

[32] The vertical mixing from current shear is too weak to produce a reasonable seasonal thermocline, results in a large cold temperature bias and an unrealistic seasonal cycle in the subsurface in the extratropical ocean. The simulated vertical mixing is greatly enhanced in the experiments with the effect of surface waves. Accordingly, the temperature structure and seasonal cycle in these experiments are significantly improved compared with the experiment without surface waves. It is interesting that the simulated temperature structures are very similar in the two experiments with and without the shear effect, when surface waves are incorporated into the model. This suggests that the combined mixing from surface waves and buoyancy can sustain a reasonable temperature structure in upper ocean, and that the effect from the vertical shear is insignificant.

[33] Our numerical experiments revealed that surface waves play an important role in enhancing vertical mixing in the upper ocean, and their induced mixing is much more important than that from the vertical shear of the mean current especially in the extratropical ocean. In order to simulate accurately the upper ocean, it is therefore necessary to include the nonbreaking surface wave–induced vertical mixing in ocean circulation models.

[34] **Acknowledgments.** We express our sincere thanks to Academician Professor Jiping Chao, National Marine Environmental Forecasting Center of China, who initiated the idea to close the shear-induced vertical mixing. F.L.Q. was supported by the Key Project of National Natural Science Foundation of China through grant 40730842 and the Public Science and Technology Research Funds Projects of Ocean 201105019. C.J.H. was supported by the National Natural Science Foundation of China through grant 40806017 and the National Basic Research Program of China (973 Program) through grant 2010CB950500.

References

Agrawal, Y. C., E. A. Terray, M. A. Donelan, P. A. Hwang, A. J. Williams III, W. M. Drennan, K. K. Kahma, and S. A. Kitaigorodskii (1992), Enhanced dissipation of kinetic energy beneath surface waves, *Nature*, *359*, 219–220, doi:10.1038/359219a0.

Alford, M. H. (2003), Improved global maps and 54-year history of wind-work on ocean inertial motions, *Geophys. Res. Lett.*, *30*(8), 1424, doi:10.1029/2002GL016614.

Anis, A., and J. N. Moum (1995), Surface wave-turbulence interactions: Scaling ε(*z*) near the sea surface, *J. Phys. Oceanogr.*, *25*, 2025–2045, doi:10.1175/1520-0485(1995)025<2025:SWISNT>2.0.CO;2.

Babanin, A. V., and B. K. Haus (2009), On the existence of water turbulence induced by non-breaking surface waves, *J. Phys. Oceanogr.*, *39*, 2675–2679, doi:10.1175/2009JPO4202.1.

Blumberg, A. F., and G. L. Mellor (1987), A description of a three-dimensional coastal ocean circulation model, in *Three-Dimensional Coastal Ocean Models*, *Coastal Estuarine Stud.*, vol. 4, edited by N. Heaps, pp. 1–16, AGU, Washington, D. C., doi:10.1029/CO004p0001.

Chen, D., A. J. Busalacchi, and L. M. Rothstein (1994), The roles of vertical mixing, solar radiation, and wind stress in a model simulation of the sea surface temperature seasonal cycle in the tropical Pacific Ocean, *J. Geophys. Res.*, *99*(C10), 20,345–20,359, doi:10.1029/94JC01621.

Cheung, T. K., and R. L. Street (1988), The turbulent layer in the water at an air-water interface, *J. Fluid Mech.*, *194*, 133–151, doi:10.1017/S0022112088002927.

Collard, F., F. Ardhuin, and B. Chapron (2009), Monitoring and analysis of ocean swell fields from space: New methods for routine observations, *J. Geophys. Res.*, *114*, C07023, doi:10.1029/2008JC005215.

Conkright, M. E., R. A. Locarnini, H. E. Garcia, T. O'Brien, T. P. Boyer, C. Stephens, and J. I. Antonov (2002), World Ocean Atlas 2001: Objective analyses, data statistics, and figures [CD-ROM], *Internal Rep. 17*, 17 pp., Natl. Oceanogr. Data Cent., Silver Spring, Md.

Craig, P. D., and M. L. Banner (1994), Modeling wave-enhanced turbulence in the ocean surface layer, *J. Phys. Oceanogr.*, *24*, 2546–2559, doi:10.1175/1520-0485(1994)024<2546:MWETIT>2.0.CO;2.

Crawford, W. R., and T. R. Osborn (1979), Microstructure measurements in the Atlantic Equatorial Undercurrent under GATE, *Deep Sea Res., Part A*, *26*, suppl. II, 285–308.

da Silva, A., A. C. Young, and S. Levitus (Eds.) (1994), *Atlas of Surface Marine Data 1994*, vol. 1, *Algorithms and Procedures*, 83 pp., NOAA, Silver Spring, Md.

Dai, D. J., F. Qiao, W. Sulisz, L. Han, and A. Babanin (2010), An experiment on the non-breaking surface-wave-induced vertical mixing, *J. Phys. Oceanogr.*, *40*, 2180–2188, doi:10.1175/2010JPO4378.1.

Drennan, W. M., M. A. Donelan, E. A. Terray, and K. B. Katsaros (1996), Oceanic turbulence dissipation measurements in SWADE, *J. Phys. Oceanogr.*, *26*, 808–815, doi:10.1175/1520-0485(1996)026<0808:OTDMIS>2.0.CO;2.

Ezer, T. (2000), On the seasonal mixing layer simulated by a basin-scale ocean model and the Mellor-Yamada turbulence scheme, *J. Geophys. Res.*, *105*, 16,843–16,855, doi:10.1029/2000JC900088.

Huang, C. J., F. Qiao, and Z. Song (2008), The effect of the wave-induced mixing on the upper ocean temperature in a climate model, *Acta Oceanol. Sin.*, *27*(3), 104–111.

Huang, C. J., F. Qiao, Z. Song, and T. Ezer (2011), Improving simulations of the upper ocean by inclusion of surface waves in the Mellor-Yamada turbulence scheme, *J. Geophys. Res.*, *116*, C01007, doi:10.1029/2010JC006320.

Huang, R. X. (1999), Mixing and energetics of the oceanic the thermohaline circulation, *J. Phys. Oceanogr.*, *29*, 727–746, doi:10.1175/1520-0485(1999)029<0727:MAEOTO>2.0.CO;2.

Kara, A. B., A. J. Wallaraft, and H. E. Hurlburt (2003), Climatological SST and MLD predictions from a global layered ocean model with an embedded mixed layer, *J. Atmos. Oceanic Technol.*, *20*, 1616–1632, doi:10.1175/1520-0426(2003)020<1616:CSAMPF>2.0.CO;2.

Large, W. G., J. C. McWilliams, and S. C. Doney (1994), Oceanic vertical mixing: A review and a model with a nonlocal boundary layer parameterization, *Rev. Geophys.*, *32*, 363–403, doi:10.1029/94RG01872.

Li, X., Y. Chao, J. C. McWilliams, and L.-L. Fu (2001), A comparison of two vertical-mixing schemes in a Pacific Ocean general circulation model, *J. Clim.*, *14*, 1377–1398, doi:10.1175/1520-0442(2001)014<1377:ACOTVM>2.0.CO;2.

Lin, X. P., S. P. Xie, X. Chen, and L. Xu (2006), A well-mixed warm water column in the central Bohai Sea in summer: Effects of tidal and surface wave mixing, *J. Geophys. Res.*, *111*, C11017, doi:10.1029/2006JC003504.

Maes, C., G. Mades, and P. Delecluse (1997), Sensitivity of an equatorial Pacific OGCM to the lateral diffusion, *Mon. Weather Rev.*, *125*, 958–971, doi:10.1175/1520-0493(1997)125<0958:SOAEPO>2.0.CO;2.

Martin, P. J. (1985), Simulation of the mixed layer at OWS November and Papa with several models, *J. Geophys. Res.*, *90*, 903–916, doi:10.1029/JC090iC01p00903.

Matsuno, T., J.-S. Lee, M. Shimizu, S.-H. Kim, and I. C. Pang (2006), Measurements of the turbulent energy dissipation rate E and an evaluation of the dispersion process of the Changjiang Diluted Water in the East China Sea, *J. Geophys. Res.*, *111*, C11S09, doi:10.1029/2005JC003196.

Mellor, G., and T. Yamada (1982), Development of a turbulence closure model for geophysical fluid problems, *Rev. Geophys.*, *20*, 851–875, doi:10.1029/RG020i004p00851.

Milliff, R. F., J. Morzel, D. B. Chelton, and M. H. Freilich (2004), Wind stress curl and wind stress divergence biases from rain effects on QSCAT surface wind retrievals, *J. Atmos. Oceanic Technol.*, *21*, 1216–1231, doi:10.1175/1520-0426(2004)021<1216:WSCAWS>2.0.CO;2.

Pacanowski, R. C., and S. G. H. Philander (1981), Parameterization of vertical mixing in numerical models of tropical oceans, *J. Phys. Oceanogr.*, *11*, 1443–1451, doi:10.1175/1520-0485(1981)011<1443:POVMIN>2.0.CO;2.

Paulson, C. A., and J. J. Simpson (1977), Irradiance measurements in the upper ocean, *J. Phys. Oceanogr.*, *7*, 952–956, doi:10.1175/1520-0485(1977)007<0952:IMITUO>2.0.CO;2.

Pezzi, L. P., and K. J. Richards (2003), Effects of lateral mixing on the mean state and eddy activity of an equatorial ocean, *J. Geophys. Res.*, *108*(C12), 3371, doi:10.1029/2003JC001834.

Phillips, O. M. (1961), A note on the turbulence generated by gravity waves, *J. Geophys. Res.*, *66*(9), 2889–2893, doi:10.1029/JZ066i009p02889.

Pleskachevsky, A., M. Dobrynin, A. V. Babanin, H. Gunther, and E. Stanev (2011), Turbulent mixing due to surface waves indicated by remote sensing of suspended particulate matter and its implementation into coupled modeling of waves, turbulence, and circulation, *J. Phys. Oceanogr.*, *41*, 708–724, doi:10.1175/2010JPO4328.1.

Qiao, F., Y. Yuan, Y. Yang, Q. Zheng, C. Xia, and J. Ma (2004), Wave-induced mixing in the upper ocean: Distribution and application to a global ocean circulation model, *Geophys. Res. Lett.*, *31*, L11303, doi:10.1029/2004GL019824.

Qiao, F., Y. Yuan, T. Ezer, C. Xia, Y. Yang, X. Lü, and Z. Song (2010), A three-dimensional surface wave-ocean circulation coupled model and its initial testing, *Ocean Dyn.*, *60*(5), 1339–1355, doi:10.1007/s10236-010-0326-y.

Rapp, R. J., and W. K. Melville (1990), Laboratory measurements of deep-water breaking waves, *Philos. Trans. R. Soc. London, Ser. A*, *331*, 735–800, doi:10.1098/rsta.1990.0098.

Shu, Q., F. Qiao, Z. Song, C. Xia, and Y. Yang (2011), Improvement of MOM4 by including surface wave-induced vertical mixing, *Ocean Modell.*, *40*, 42–51, doi:10.1016/j.ocemod.2011.07.005.

Smagorinsky, J. (1963), General circulation experiments with the primitive equations: I. The basic experiment, *Mon. Weather Rev.*, *91*, 99–164, doi:10.1175/1520-0493(1963)091<0099:GCEWTP>2.3.CO;2.

Snodgrass, F. E., G. W. Groves, K. F. Hasselmann, G. R. Miller, W. H. Munk, and W. H. Powers (1966), Propagation of ocean swell across the Pacific, *Philos. Trans. R. Soc. London, Ser. A*, *259*, 431–497, doi:10.1098/rsta.1966.0022.

Teixeira, M. A. C., and S. E. Belcher (2002), On the distortion of turbulence by a progressive surface wave, *J. Fluid Mech.*, *458*, 229–267, doi:10.1017/S0022112002007838.

Teng, Y., Y. Yang, F. Qiao, and J. Lu (2009), Energy budget of surface waves in the global ocean, *Acta Oceanol. Sin.*, *28*(3), 5–10.

Wang, W., and R. X. Huang (2004a), Wind energy input to the surface waves, *J. Phys. Oceanogr.*, *34*, 1276–1280, doi:10.1175/1520-0485(2004)034<1276:WEITTS>2.0.CO;2.

Wang, W., and R. X. Huang (2004b), Wind energy input to the Ekman layer, *J. Phys. Oceanogr.*, *34*, 1267–1275, doi:10.1175/1520-0485(2004)034<1267:WEITTE>2.0.CO;2.

Wang, Y., F. Qiao, G. Fang, and Z. Wei (2010), Application of wave-induced vertical mixing to the K profile parameterization scheme, *J. Geophys. Res.*, *115*, C09014, doi:10.1029/2009JC005856.

Watanabe, M., and T. Hibiya (2002), Global estimate of the wind-induced energy flux to the inertial motion in the surface mixed layer, *Geophys. Res. Lett.*, *29*(8), 1239, doi:10.1029/2001GL014422.

Wunsch, W. (1998), The work done by the wind on the oceanic general circulation, *J. Phys. Oceanogr.*, *28*, 2332–2340, doi:10.1175/1520-0485(1998)028<2332:TWDBTW>2.0.CO;2.

Xia, C., et al. (2006), Three-dimensional structure of the summertime circulation in the Yellow Sea from a wave-tide-circulation model, *J. Geophys. Res.*, *111*, C11S03, doi:10.1029/2005JC003218.

Yang, Y., F. Qiao, Y. Teng, and Y. Yuan (2005), MASNUM ocean wave model in spherical coordinate and its application, *Acta Oceanol. Sin.*, *27*, 1–7.